Finite Element Analysis of Laser-Generated Rayleigh Wave Scattering by Cracks in a Plate*

Guan Jianfei, Shen Zhonghua, Xu Baiqiang, Ni Xiaowu**, Lu Jian
Department of Applied Physics, Nanjing University of Science & Technology, Nanjing 210094

Abstract The finite element method has been utilized to investigate the transient scattering of Rayleigh wave by a crack on a plate. The incident wave models and the guided waves generated by a pulsed line source are laser irradiation on the plate. Three surface-breaking cracks and three subsurface cracks are studied here. The results show that the location and the depth of cracks have measurable effects on the surface responses in time domains. The deeper surface-breaking crack will generate the more amplitude reflected wave, and the effect of the subsurface crack attributes to the vertical distance from the tip of subsurface crack to the top surface of the plate. Therefore, the waveform can be used to detect the surface breaking crack dimensions and the location position of the subsurface crack.

Keywords Laser-generated; Rayleigh waves; Finite element method; Surface-breaking cracks
CLCN TN249; O426 **Document Code** A

0 Introduction

Conventional ultrasonic inspection utilizes the transducer to generate ultrasound, which has to touch the structural surface and has poor bandwidth. Laser ultrasonic generates great hopes within the field of non-destructive evaluation (NDE) due to its non-contact feature in the measuring process and the ability of broadband signal generation[1~4].

Ultrasound generated by a pulsed laser source can occur by various mechanisms including the photothermoelastic effect, which does not damage the surface[5,6]. When the incident wavelength is comparable to the structure thickness, the guided wave generated in a plate-like structure is called a Lamb wave[7,8]. When the thickness of the plate increases, the guide wave is generated in Rayleigh waveform[9]. It is well known that a Rayleigh type surface wave is a non-dispersive wave propagating on the surface of homogenous elastic half-space and its amplitude decreases with depth. Using this wave to determine the characteristics of surface-breaking crack and subsurface flaws seems to be an attractive mean to approach the problem. Generally, a point source has been used for most practical applications[10]. While in certain cases, it is advantageous to use a laser line source rather than a point, for example, to enhance the wave directivity; in addition, the description of a laser line source is simplified since the system model can be reduced to two dimensional, thus eliminating some associated mathematical complexity.

In this work, the displacements generated by a laser line source are calculated using the finite element method. The finite element method (FEM) is a good way for solving this problem because it has the capability in finding a feasible solution for a structure, which has the complex geometries or various defects. The displacement at any location in the plate can be easily obtained by the finite element method. Xu et al. have calculated the Laser-generated surface acoustic waves in single Al plate[11] and coating-substrate system[12] successfully by the finite element method. This paper concentrates on the surface of the plate for in the thermoelastic regime a laser source allots more energy to the Rayleigh wave than the longitudinal wave. This means that thermoelastically generated Rayleigh waves have greater amplitude than longitudinal waves. The obvious amplitude and the broad frequency components make it more desirable for using in flaw detection systems.

1 Theory model

1.1 Thermal conductive theory

A piece of Al plate is illuminated by a laser line source in normal direction and the geometry is schematically shown in Fig. 1. The thickness of the plate is denoted by h, and $x = l$ represents the

*Supported by the National Natural Science Foundation (No. 60208004) and Natural Science Foundation of Jiangsu Province, (No. BK2001056) and the Teaching and Research Award Program for Outstanding Young Professor in Higher Education Institute. MOE, P. R. C
** Tel: 025-84315075 Email: nxw@mail.njust.edu.cn
Received date: 2004-06-25

location of the surface-breaking crack. The dimension of the defect and the energy distribution of the laser beam are uniform in the z-axis direction. We can analyze the x-y plane of the specimen as shown in Fig. 2. Therefore, the three

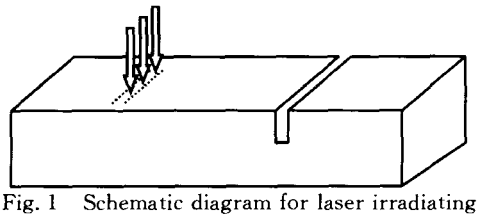

Fig. 1 Schematic diagram for laser irradiating spectimen plate

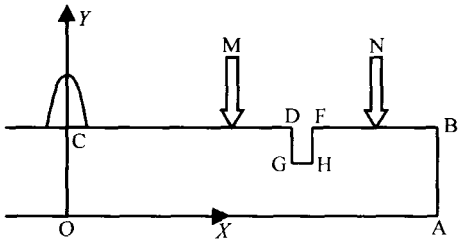

Fig. 2 Schematic diagram of the computing model

dimensions Cartesian coordinated can be reduced to two dimensions, and the thermal conductive equation can be described as

$$\rho c \frac{\partial T(x,y,t)}{\partial t} = \frac{\partial}{\partial x}\left(k_x \frac{\partial T(x,y,t)}{\partial x}\right) + \frac{\partial}{\partial y}\left(k_y \frac{\partial T(x,y,t)}{\partial y}\right) \quad (1)$$

where $T(x, y, t)$ represents the temperature distribution at the time of t. ρ, c and k are the density, thermal capacity and thermal conductive coefficients.

The boundary conditions can be expressed as

$$-k_y \frac{\partial T(x,y,t)}{\partial y}\Big|_{y=h} = I_0(1-R)f(x)g(t) \quad (2)$$

and

$$\frac{\partial T(x,y,t)}{\partial y}\Big|_{y=0} = 0 \quad (3)$$

where R denotes the reflectivity of the surface of the sample. The h represents the thickness of the sample. I_0 is the incident laser intensity. $f(x)$ and $g(t)$ are the spatial and temporal distribution of the laser pulse. In our computing model, the two functions form can be expressed as

$$f(x) = \exp\left(-\frac{x^2}{a_0^2}\right) \text{and } g(t) = \frac{t}{t_0^2}\exp\left(-\frac{t}{t_0}\right) \quad (4)$$

where the a_0 is the half-width of the line source, and the t_0 is the rise time of the laser pulse.

1.2 Thermoelastic theory of laser ultrasound

When the specimen surface is illuminated by a pulse laser with the energy less than the melting threshold of the specimen, a transient displacement field will be excited due to the thermoelastic expansion. In the thermoelastic body, the displacement satisfies

$$(\lambda+2\mu)\nabla(\nabla \cdot U) - \mu\nabla\times\nabla\times U - \alpha(3\lambda+2\mu)\nabla T(x,y,t) = \rho\frac{\partial^2 U}{\partial^2 t} \quad (5)$$

where $U(x, y, t)$ is the time-dependent displacement. λ and μ are the Lamé constants. ρ is the density and α is the thermal expansion coefficient of the isotropic plate materials. The boundary conditions at the top surface $y=h$ can be expressed as

$$\boldsymbol{n}[\boldsymbol{\sigma} - (3\lambda+2\mu)\alpha T(x,y,t)\boldsymbol{I}] = 0 \quad (6)$$

where $\boldsymbol{n}$ is the unit vector normal to the surface. $\boldsymbol{I}$ is the unit tensor and $\boldsymbol{\sigma}$ is the stress tensor. And the three edges of the crack are adapted to free boundary condition too. An absorbing boundary condition[11] was imposed on the left, right and bottom edges of the rectangle.

In addition to the boundary condition, there is also an initial condition

$$U(x,y,t) = \frac{\partial U(x,y,t)}{\partial t} = 0, t = 0 \quad (7)$$

2 Numerical analysis

2.1 Laser parameters and material characteristics

Based on the theories described above, we have constructed the finite element model accordingly. It is clear that the element size of 20 μm is good enough to capture both the incident and reflected surface acoustic waves. In our model, for the location surface breaking crack l = 15 mm was considered; and three cracks with different depths are used, their depths are 2 mm, 4 mm and 8 mm with the same width of 0.2 mm, named crack Ⅰ, crack Ⅱ and crack Ⅲ, respectively. For the subsurface cracks, they are embedded underneath the top surface of the Al plate by 0.5 mm, 1.0 mm and 1.5 mm respectively and their dimensions are taken as the same as crack Ⅰ.

The laser energy is 0.75 mJ, and the pulse rise time t_0 and the half width of the laser line source are taken to be 10 ns and 300 μm, respectively. The temperature dependence of the all kinds of parameters of the aluminum can be found in literature[9], which are necessary to the thermal analysis, and included the coefficients of light energy absorption, thermal conductivities, the specific heat capacities and density[12]. The mechanical properties of aluminum in the calculation can also be found in ref. [12].

2.2 Numerical method

The simulation model is the profile of a aluminum block, and has the dimensions, 60 mm×

20 mm, in the x-, y-coordinate dimensions, respectively as shown in Fig. 2.

The surface acoustic wave is generated at $x=0$ mm by the pulsed laser with the energy 0.75 mJ and propagates towards the crack, which is located at $x=15$ mm. The classical thermal conduction equation for finite element model can be expressed as

$$[K]\{T\}+[C]\{\dot{T}\}=\{p_1\}+\{p_2\} \quad (8)$$

with the heat capacity matrix $[C]$, the conductivity matrix $[K]$, the heat flux vector $\{p_1\}$ and the heat source vector $\{p_2\}$, where $\{T\}$ is the temperature vector, and $\{\dot{T}\}$ is the temperature rate vector. For wave propagations, and ignoring damping, the governing finite element equations are

$$[M]\{\ddot{U}\}+[S]\{U\}=\{F_{ext}\} \quad (9)$$

where $[M]$ is the mass matrix, $[S]$ is the stiffness matrix, $\{U\}$ is the displacement vector, $\{\ddot{U}\}$ is the acceleration vector and $\{F_{ext}\}$ is the external force vector.

It should be noted that equilibrium equations (11) and (12) are established only at a particular time t, and the entire time history of generalized displacement $\{U\}$ can be obtained through the procedure given in ref. [9], in which a time integration over whole time has been performed.

2.3 Numerical results

2.3.1 *The results of the surface-breaking crack*

The effect of depth of surface breaking crack was found to be quite noticeable in the normal surface displacement. Generally, it was found that the effect of crack was mostly pronounced in the near field. So we focus our attention on the near field response. The laser source is located at $x=0$ mm on the top surface, and the two receivers points M, N are positioned at $x=10$ mm and $x=20$ mm respectively. Meanwhile, the front side DG of the surface-breaking crack is located at $x=15$ mm on the top surface of the plate, so that both of the two receivers points keep the 5mm-length distance to the front side of the crack.

In order to understand the effect due to the presence of the crack, the vertical surface displacements for the case without a crack are shown in Fig. 3. Note, as a reference, Fig. 3 also shows that the response at $x=15$ mm when there is no cracks by thick solid lines. The main features of the surface acoustic waves are three kinds of waves. One is the surface skimming longitudinal wave denoted by sP, which is an out-ward displacing mono-polar wave. The other two are the surface shear wave fronts denoted by sS and the main initially negative-going dipolar Rayleigh wave denoted by R.

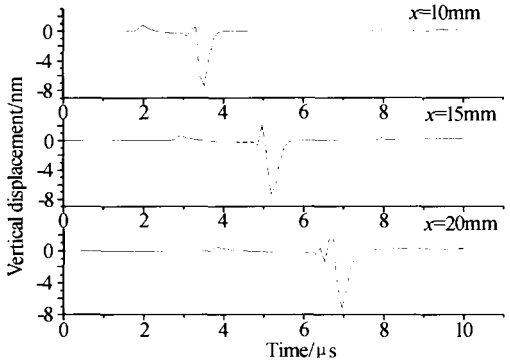

Fig. 3 The vertical surface displacements of the Al Plate without crack

When the pulsed laser illuminated on the top surface of the plate with the surface-breaking crack, the vertical surface displacements of the two receivers are shown in Fig. 4 and 5. Comparing the time-domain responses of the receive point M to the three cracks shown in Fig. 4, the amplitudes of the reflected wave in the presence of crack Ⅲ have largest magnitudes, while the crack Ⅰ produce the reflected wave with the smallest amplitude. So there is more reflected energy from the deeper surface crack, which can help us to analysis the depth of the surface crack by measuring the amplitudes of the reflected wave.

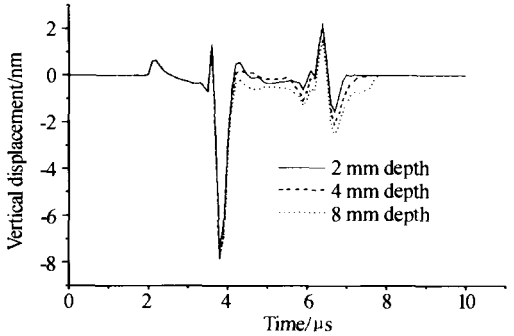

Fig. 4 The reflected surface wave from the three surface breaking cracks with 2 mm, 4 mm, 8 mm depth

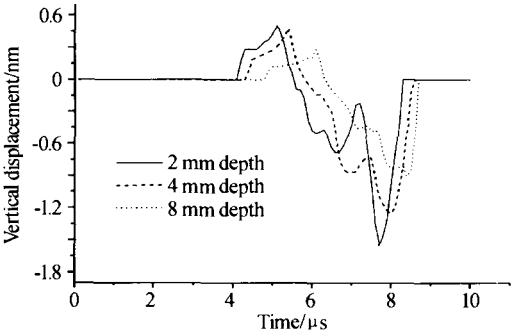

Fig. 5 The transmitted surface wave through the three surface breaking cracks with 2 mm, 4 mm, 8 mm depth

On the other hand, it is clearly that the amplitudes in the presence of crack Ⅲ have lowest amplitude in the transmitted waves from Fig. 5, while there is highest amplitudes of transmitted wave which has passed through the crack Ⅰ. This phenomenon seems to imply that a portion of Rayleigh wave is reflected back, and its contribution to the transmitted Rayleigh wave becomes smaller and smaller as the depth of the surface crack increases.

From two points quoted above, we can confirm a further conclusion that the Rayleigh wave mainly propagates on the surface of the plate, and the depth of the R-wave penetration depends on its central frequency. For a surface-breaking crack, when the crack depth is short, compared with the central band wavelength of the initial R wave, the low frequencies of the initial wave have significant energy below the crack and are therefore directly transmitted. So the laser-generated Rayleigh wave with different central frequency will have various abilities to detect the surface breaking crack with different depths. Meanwhile the central frequency of the initial Rayleigh wave is dependent on the parameter of the laser pulse.

At the same time, it can be found further from Fig. 5 that the transmitted Rayleigh wave arrives much latter while the surface crack is deeper. From this we can draw a conclusion that the length of time which Rayleigh wave passed the crack, is correlative with the dimension of the crack. Just as mentioned in the literature[13]: it is found that different depth of surface-breaking crack caused different delays in arrivals of the peaks in the displacements. So we can attain approximately the depth of the surface-breaking crack from the delay time, which is cost by the interaction of the Rayleigh wave and the surface-breaking crack.

2.3.2 *The results of the subsurface defects*

For the subsurface crack, the transient response of the transmitted signal shown in Fig. 7 is similar to the case without crack shown in Fig. 3. However, the effect of the crack still can be seen obviously from the amplitudes of the reflected waves received in the front of the crack, which is shown in Fig. 6. In this figure, the smaller amplitude of the reflected wave can be observed when the subsurface defect was buried deeper. It is due to the fact that only the low frequency components of the initial Rayleigh wave is affected by the subsurface defect. So the deeper the subsurface defect is buried, the fewer frequency components of the initial Rayleigh wave will be affected, and the reflected waves have smaller amplitude.

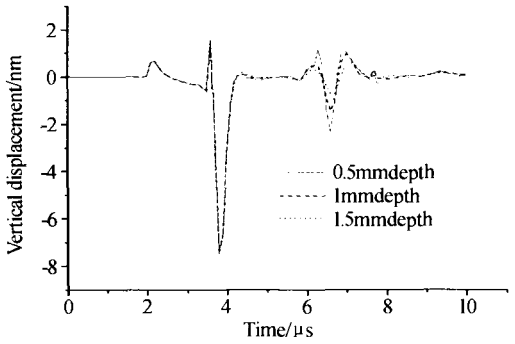

Fig. 6 The reflected surface wave from the three subsurface creaks buried in 0.5 mm, 1 mm, 1.5 mm depth

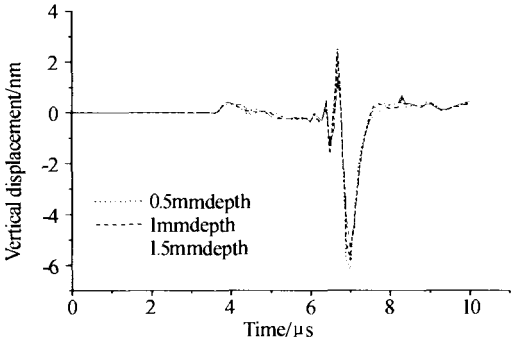

Fig. 7 The transmitted waves through the three subsurface creaks buried in 0.5 mm, 1 mm, 1.5 mm depth

It is well known that the Rayleigh wave decays with the depth in the order of several wavelengths. Therefore, when the distance from the surface of plate to the tip of subsurface defect reaches or exceeds the central wavelength of the Rayleigh wave, we cannot observe the reflected R wave clearly. That is to say, in this case, we cannot detect the subsurface defect only through the Rayleigh wave.

3 Conclusions

Six different cracks including three surface-breaking cracks with different depth and three subsurface crack buried in different depth, are studied here. It is found that the effects of the these cracks cause different responses in time domains, and the deeper surface breaking crack is found to cause larger amplitude of the back-scattered field. In addition, these different depths of surface breaking crack cause different delays in arrivals of the peaks in the forward scattered responses displacement. These differences can be used to estimate the differences between crack depths. On the other hand, there are distinct

differences in the responses because of the surface-breaking cracks and subsurface cracks, particularly in the transmitted waveforms. The displacement at any location in the plate can be easily obtained by the finite element method.

References

1 Shen Z H, Zhang S Y, Chen J C. Theory study on surface acoustic wave generated by a laser pulse. *Analytical Science*, 2001, **17**: 204～207

2 Cheng J C, Zhang S Y. Quantitative theory for laser-generated lamb waves in orthotropic thin plates. *Appl Phys Lett*, 1999, **74**(14): 2087～2089

3 Queheillalt D T, Lu Y, Haydn N G. Laser ultrasonic studies of solid-liquid interfaces. *J Acoust Soc Am*, 1997, **101**(2): 843～853

4 Ghosh T, Kundu T, Karpur P. Efficient use of Lamb modes for detecting defects in large plates. *Ultrasonics*, 1998, **36**(7): 791～801

5 Zheng Ruilun, Liu Jun. Thermodynamic effect of the metal material face irradiated by strong laser. *Acta Photonica Sinica*, 2003, **31**(4): 480～484

6 Liu Shunfa, Cheng Hongbin. Calculatng the temperature field of 3-D object heated by laser. *Acta Photonica Sinica*, 2000, **29**(3): 267～270

7 Younho Cho, Joseph L Rose. An elastodynamic hybrid boundary element study for elastic guided wave interactions with a surface-breaking defect. *Int J Solids and Structures*, 2000, **37**(20): 4103～4124

8 Zhao Xiaoliang, Rose J L. Boundary element modeling for defect characterization potential in a wave guide. *Int J Solids and Structures*, 2003, **40**(11): 2645～2658

9 Hevin G, Abraham O. Characterisation of surface cracks with Rayleigh waves: a numerical model. *NDE & E International*, 1998, **31**(4): 289～297

10 Rose L R F. Point-source representation for laser-generated ultrasound. *J Acoust Soc Am*, 1984, **75**(3): 723～732

11 Xu B Q, Shen Z H, Ni X W, *et al*. Numerical simulation of laser-induced ultrasonic by finite element method. *J Appl Phys*, 2004, **95**(2): 2116～2122

12 Xu B Q, Shen Z H, Ni X W, *et al*. Finite element model of laser-generated surface acoustic waves in coating-substrate system. *J Appl Phys*, 2004, **95**(2): 2109～2115

13 Datta D, Kishore N N. Features of ultrasonic wave propagation to identify defects in composite materials modeled by finite element method. *NDT&E International*, 1996, **29**(4): 213～223

14 Zheng R L. Temperature rise and temperature rise rate of metal plate by laser radiation. *Acta Chemica Sinica*, 1998, **27**(11): 1028～1032

15 Liu S W, Datta S K. Scattering of ultrasonic wave by cracks in a plate. *J Appt Mech*, 1993, **60**: 352～357

激光激发声表面波在缺陷板材中散射过程的有限元分析

关建飞 沈中华 许伯强 倪晓武 陆 建

(南京理工大学应用物理系, 南京 210094)

收稿日期: 2004-06-25

摘 要 利用有限元法模拟了金属板材中激光激发的声表面波经过缺陷位置时发生散射的瞬态过程, 采用线状激光源作为超声导波的激发源. 针对三种不同深度的表面缺陷以及三种亚表面缺陷的模型进行了对比计算, 结果显示缺陷的深度及位置对声表面波的时域特征存在显著的影响. 表面缺陷深度越深将产生较大幅度的表面反射回波, 亚表面缺陷的影响将取决于缺陷上顶面距离板材上表面的距离. 因此, 数值模拟结果表明通过分析激光产生的表面波形可以判定近表面缺陷的尺寸和所处的位置.

关键词 激光激发; 瑞利波; 有限元; 表面缺陷

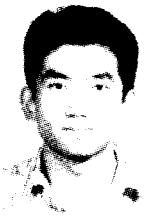

Guan Jianfei was born in April 1979, Shanxi Province. He is a doctoral graduate in Optics Engineering in Department of Applied Physics, Nanjing University of Science & Technology. His research interests are laser generated ultrasound and its applications to nondestructive evaluation.